

Ergodicity test of the eddy-covariance technique

Jinbei CHEN¹ Yinqiao HU² Ye YU Shihua LÜ

Key Laboratory of Land Surface Processes and Climate Change in Cold and Arid Regions; Cold and Arid Regions Environment and Engineering Institute, Chinese Academy of Sciences, Lanzhou 730000, P R China.

Pingliang Land Surface Process & Severe Weather Research Station, Chinese Academy of Science, Pingliang 744015, P R China.

1 E-mail: chenjinbei@lzb.ac.cn

2 Corresponding author: hyq@ns.lzb.ac.cn

Abstract

The ergodic hypothesis is a basic hypothesis typically invoked in atmospheric surface layer (ASL) experiments. The ergodic theorem of stationary random processes is introduced to analyze and verify the ergodicity of atmospheric turbulence measured using the eddy-covariance technique with two sets of field observational data. The results show that the ergodicity of atmospheric turbulence in ABL is not only relative to the atmospheric stratification but also to the eddy scale of atmospheric turbulence. The eddies of atmospheric turbulence, of which the scale is smaller than the scale of the atmospheric boundary layer (ABL), i.e., the spatial scale is less than 1,000 m and temporal scale is shorter than 10 min, effectively satisfy the ergodic theorems. Under these restrictions, a finite time average can be used as a substitute for the ensemble average of atmospheric turbulence. Whereas, eddies that are larger than ABL scale dissatisfy the mean ergodic theorem. Consequently, when a finite time average is used to substitute for the ensemble average, the eddy-covariance technique incurs large errors due to the loss of low frequency information associated with larger eddies. A multi-stations observation is compared with a single-station, and then the scope that satisfies the ergodic theorem is extended from scales smaller than the ABL approximately 1000 m to scales greater than that about 2000 m. Therefore, the calculation results of averages, variances and fluxes of turbulence are more faithfully approximate the actual values due to effectively satisfy the ergodic assumption. Regardless of vertical velocity or temperature, the variance of eddies at different scales follows Monin-Obukhov Similarity Theory (MOST) better if the ergodic theorem can be satisfied, if not it deviates from MOST. The exploration of ergodicity in atmospheric turbulence is doubtlessly helpful in understanding the issues in

35 atmospheric turbulent observations, and provides a theoretical basis for overcoming
36 related difficulties.

37 **Keywords:** Atmospheric turbulence; Ergodic hypothesis; eddy-covariance technique;
38 Monin-Obukhov similarity theory (MOST); atmospheric surface layer (ASL)

39

40 **1 Introduction**

41 The basic principle of average of the turbulence measurements is based on ensembles
42 averaged over space, time and state. However, it is impossible to make an actual
43 turbulence measurement with enough observational instruments in space for sufficient
44 time to obtain all states of turbulent eddies to achieve the goal of an ensemble average.
45 Therefore, based on the ergodic hypothesis, the time average of one spatial point,
46 taken over a sufficiently long observational time, is used as a substitute for the
47 ensemble average for temporally steady and spatially homogeneous surfaces (Stull
48 1988; Wyngaard 2010; Aubinet 2012). The ergodic hypothesis is a basic assumption
49 in turbulence experiments in the atmospheric boundary layer (ABL) and atmospheric
50 surface layer (ASL). Stationarity, homogeneity, and ergodicity are routinely used to
51 link ensemble statistics (mean and higher-order moments) of field experiments in the
52 ABL. Many authors habitually refer to the ergodicity assumption with descriptions
53 such as “when satisfying ergodic hypothesis.....” or “something indicates that
54 ergodic hypothesis is satisfied”. The success of Monin-Obukhov Similarity Theory
55 (MOST) for unstable and near-neutral conditions is just evidence of the validity of the
56 ergodic hypothesis in the ASL. While ergodicity is only a necessary condition for the
57 success of MOST, but also it does not prove ergodicity (Katul et al. 2004). The
58 success of MOST under the conditions of stationary and homogeneity implies that the
59 stationary and homogeneity are also the important conditions of ASL ergodicity.
60 Therefore, many ABL experiments focus on seeking ideal homogeneous surfaces.
61 Some test procedures are widely applied to establish stationarity (Foken and Wichura
62 1996; Vickers and Mahrt 1997). Katul and Hsieh (1999) qualitatively analyzed the
63 ergodicity problem in atmospheric turbulence, and believed that it is common for the
64 neutral and unstable ASL to satisfy ergodicity, while it is difficult to reach ergodicity
65 in the stable ASL. Eichinger et al. (2001) indicate that LIDAR technique opens up
66 new possibilities for atmospheric measurements and analyses by providing spatial and
67 temporal atmospheric information with simultaneous high-resolution. The stationarity

68 and ergodicity can be tested for such ensembles of experiments. Recent advance in
69 LIDAR measurements offers a promising first step for direct evaluation of such
70 hypotheses for ASL flows (Higgins et al., 2013). Higgins et al. (2013) applied LIDAR
71 of water vapor concentration to investigate the ergodic hypothesis of atmospheric
72 turbulence for the first time. It is clear all the same that there is a need to reevaluate
73 the technologies of turbulence measurement, to test the ergodicity of atmospheric
74 turbulence quantitatively by means of observation experiments.

75 The ergodic hypothesis was first proposed by Boltzmann (Boltzmann 1871; Uffink
76 2004) in his study of the ensemble theory of statistical dynamics. He argued that a
77 trajectory traverses *all* points on the energy hypersurface after a certain amount of
78 time. At the beginning of 20th century, the Ehrenfest couple (Ehrenfest. and
79 Ehrenfest-Afanassjewa 1912; Uffink 2004) proposed a quasi-ergodic hypothesis and
80 changed the term “traverses *all* points” in the aforesaid ergodic hypothesis to “passes
81 arbitrarily close to every point”. The basic points of ergodic hypothesis or
82 quasi-ergodic hypothesis recognize that the macroscopic property of a system in the
83 equilibrium state is an average of microcosmic quantity in sufficient long time.
84 Nevertheless, the ergodic hypothesis or quasi-ergodic hypothesis were never proven
85 theoretically. The proof of the ergodic hypothesis in physics aroused the interest of
86 mathematicians. Famous mathematician, Neumann et al. (1932) first theoretically
87 proved the ergodic theorem in topological space (Birkhoff 1931, Krengel 1985).
88 Afterward, a banausic ergodic theorem of stationary random processes was proved to
89 provide a necessary and sufficient condition for the ergodicity of stationary random
90 processes. Mattingly (2003) reviewed the research progress on ergodicity for
91 stochastically force Navier-Stokes equation, and that Galanti and Tsinober (2004) and
92 Lennaert et al. (2006) solved the Navier-Stokes equation by numerical simulation to
93 prove that turbulence that is temporally steady and spatially homogeneous is ergodic.
94 However, Galanti and Tsinober (2004) also indicated that such partially turbulent
95 flows acting as mixed layer, wake flow, jet flow, flow around the boundary layer may
96 be non-ergodic.

97 Obviously, the advances of research on ergodicity in the mathematics and physics
98 have led the way for the atmospheric sciences. We try first to introduce the ergodic
99 theorem of stationary random processes to the atmospheric turbulence in this paper.
100 The ergodicity of different scale eddies of atmospheric turbulence is directly analyzed

101 and verified quantitatively on the basis of field observation data obtained using
 102 eddy-covariance technique in the ASL.

103 **2 Theories and methods**

104 **2.1 Ergodic theorems of stationary random processes**

105 Stationary random processes are processes which will not vary with time, i.e., for
 106 observed quantity A , its function of space x_i and time t_i satisfies the following
 107 condition:

$$108 \quad A(x_1, x_2, \dots, x_n; t_1, t_2, \dots, t_n) = A(x_1, x_2, \dots, x_n; t_1 + \tau, t_2 + \tau, \dots, t_n + \tau), \quad (1)$$

109 where τ is a time period, defined as the relaxation time.

110 The mean μ_A of a random variable A and its autocorrelation function $R_A(\tau)$ are
 111 respectively defined as following:

$$112 \quad \mu_A = \lim_{T \rightarrow +\infty} \frac{1}{T} \int_0^T A(t) dt, \quad (2)$$

$$113 \quad R_A(\tau) = \lim_{T \rightarrow +\infty} \frac{1}{T} \int_0^T A(t) A(t + \tau) dt. \quad (3)$$

114 The autocorrelation function $R_A(\tau)$ is a temporal second-order moment. In the case of
 115 $\tau=0$, the autocorrelation function $R_A(\tau)$ is the variance of random variable. A necessary
 116 and sufficient condition for the stationary random processes to satisfy the mean
 117 ergodicity is the mean ergodic function $Ero(A)$ to zero (Papoulis and Pillai 1991), as
 118 shown below:

$$119 \quad Ero(A) = \lim_{T \rightarrow \infty} \frac{1}{T} \int_0^{2T} \left(1 - \frac{\tau}{2T}\right) [R_A(\tau) - \mu_A^2] d\tau = 0. \quad (4)$$

120 The mean ergodic function $Ero(A)$ is a time integral of the difference between the
 121 autocorrelation function $R_A(\tau)$ of variable A and its mean square, μ_A^2 . If the mean
 122 ergodic function $Ero(A)$ converges to zero, then the stationary random processes will
 123 be ergodic. In other words, if the autocorrelation function $R_A(\tau)$ of variable A
 124 converges to its mean square, μ_A^2 , the stationary random processes are mean ergodic.

125 The Eq. (4) is namely mean ergodic theorem to be called as well as ergodic theorem
 126 of the *weakly* stationary processes in the mathematics. For discrete variables, Eq. (4)
 127 can be rewritten as following:

$$128 \quad Ero(A) = \lim_{n \rightarrow \infty} \sum_{i=0}^n \left(1 - \frac{\tau_i}{n}\right) [R_A(\tau_i) - \mu_A^2] = 0. \quad (5)$$

129 Eq. (5) is mean ergodic theorem of the discrete variable. Hence, Eqs. (4) or (5) can be
 130 used as a criterion to judge the mean ergodicity.

131 For the stationary random processes, the necessary and sufficient condition
 132 satisfying the autocorrelation ergodicity is the autocorrelation ergodic function $\text{Er}(A)$
 133 to zero:

$$134 \quad \text{Er}(A) = \lim_{T \rightarrow \infty} \frac{1}{T} \int_0^{2T} \left(1 - \frac{\tau'}{2T}\right) [B(\tau') - |R_A(\tau)|^2] d\tau' = 0; \quad (6a)$$

$$135 \quad B(\tau') = E \left\{ A(t + \tau + \tau') A(t + \tau') [A(t + \tau) A(t)] \right\}. \quad (6b)$$

136 Where τ' is a differential variable for entire relaxation times, and that $B(\tau')$ is temporal
 137 fourth-order moment of variable A . The autocorrelation ergodic function $\text{Er}(A)$ is a
 138 time integral of the difference between the temporal fourth-order moment $B(\tau')$ of
 139 variable A and its autocorrelation function square, $|R_A(\tau)|^2$. If the autocorrelation
 140 ergodic function $\text{Er}(A)$ converges to zero, then the stationary random processes will be
 141 of autocorrelation ergodicity, and thus the autocorrelation ergodicity means that the
 142 fourth-order moment of variable of stationary random processes will converge to
 143 square of its autocorrelation function $R_A(\tau)$. Eq. (6a) is namely autocorrelation ergodic
 144 theorem to be called as well as ergodic theorem of the *strongly* stationary processes in
 145 the mathematics. The autocorrelation ergodic function of corresponding discrete
 146 variable can be determined as following:

$$147 \quad \text{Er}(A) = \lim_{n \rightarrow \infty} \sum_{i=0}^n \left(1 - \frac{\tau'_i}{n}\right) [B(\tau'_i) - |R_A(\tau_j)|^2] = 0, \quad (7a)$$

$$148 \quad B(\tau'_i) = E \left\{ \sum_{j=0}^n A(t + \tau_j + \tau'_i) A(t + \tau'_i) [A(t + \tau_j) A(t)] \right\}. \quad (7b)$$

149 Eq. (7a) is autocorrelation ergodic theorem of the discrete variable. Hence, Eqs. (6a)
 150 or (7a) can also be used as a criterion to judge the autocorrelation ergodicity.

151 The stationary random processes conform to the criterion, Eqs. (4) or (5), then they
 152 satisfy the mean ergodic theorem, or are intituled as the mean ergodicity; the
 153 stationary random processes conform to the criterion, Eqs. (6a) or (7a), then they
 154 satisfy the autocorrelation ergodic theorem, or are intituled as the autocorrelation
 155 ergodicity. If the stationary random processes are only of mean ergodicity, they are
 156 strict ergodic or narrow ergodic. If the stationary random processes are of both the

157 mean ergodicity and autocorrelation ergodicity, they are namely wide ergodic
158 stationary random processes. It is thus clear that the ergodic random processes are
159 stationary, but the stationary processes may not be ergodic.

160 In the random process theory, calculating the mean or high-order moment function
161 requires a large amount of repeated observations to acquire a sample function $A_k(t)$. If
162 the stationary random processes satisfy the ergodic condition, then time average of a
163 sample on the whole time shaft can be used to substitute for the ensemble average.
164 Eqs. (4), (5), (6a) and (7a) can be used as the criterion to judge whether or not
165 satisfying the mean and autocorrelation ergodicity. The ergodic random processes
166 must be the stationary random processes to be defined as Eq. (1), and thus are
167 stationary in relaxation time τ . If the condition such as Eqs (4) or (5) of the mean
168 ergodicity is satisfied, then a time average in finite relaxation time τ can be used to
169 substitute for infinite time average to calculate the mean Eq. (2) of random variable;
170 similarly, the finite time average can be used for substitution to calculate the
171 covariance or variance of random variable, Eq. (3), if the condition such as Eqs. (6a)
172 or (7a) of autocorrelation ergodicity is satisfied. In a similar manner, the basic
173 principle of average of the atmospheric turbulence is the ensemble average of space,
174 time and state, and it is necessary to carry through mass observations for a long period
175 of time in the whole space. This is not only a costly observation, even is hardly
176 feasible. If the turbulence satisfies the ergodic condition, then a time average in
177 relaxation time τ by multi-stations observation, even single-station observation, can
178 substitute for the ensemble average. In fact, precondition to estimate turbulent
179 characteristic quantities and fluxes in the ABL by the eddy-covariance technique is
180 that the turbulence satisfies the ergodic condition. Therefore, conditions such as Eqs.
181 (4), (5), (6a) and (7a) will also be the criterion for testing the ergodicity and
182 authenticity of results observed by the eddy-covariance technique.

183 **2.2 Band-pass filtering**

184 The scope of spatial and temporal scale of the atmospheric turbulence, which is from
185 the dissipation range, inertial sub-range to the energy range, and further the turbulent
186 large eddy, is extremely broad (Stull 1988). In such wide spatial and temporal scope,
187 the turbulent eddies include the isotropic 3-D eddy structure of high frequency
188 turbulence and orderly coherent structure of low frequency turbulence (Li et al. 2002).
189 These eddies of different scale are also each other different in terms of their spatial

190 structure and physical properties, and even their transport characteristics are not the
 191 same. It is thus reasonable that eddies with different characteristics are separated,
 192 processed and studied using different methods (Zuo et al. 2012). A major goal of our
 193 study is to understand what type of eddy in the scale can satisfy the ergodic condition.
 194 Another goal is that the time averaging of signals measured by a single station
 195 determines accurately turbulent characteristic quantities. In order to study the
 196 ergodicity of different scale eddies, Fourier transform is used as a band-pass filtering
 197 to distinguish different scale eddy. That is to say, we compel to set the Fourier
 198 transform coefficient of the part of frequencies, which does not need, as zero, and then
 199 acquire the signals after filtering by means of Fourier inverse transformation. The
 200 specific formulae are shown below:

$$201 \quad F_A(n) = \frac{1}{N} \sum_{k=0}^{N-1} A(k) \cos\left(\frac{2\pi nk}{N}\right) - \frac{i}{N} \sum_{k=0}^{N-1} A(k) \sin\left(\frac{2\pi nk}{N}\right), \quad (8)$$

$$202 \quad A(k) = \sum_{n=a}^{N-1} F_A(n) \cos\left(\frac{2\pi nk}{N}\right) + i^2 \sum_{n=a}^{N-1} F_A(n) \sin\left(\frac{2\pi nk}{N}\right). \quad (9)$$

203 In Eqs. (8) and (9), $F_A(n)$ and $A(k)$ are respectively the Fourier transformation and
 204 Fourier inverse transformation including N data points from $k=0$ to $k=N-1$, and n is the
 205 cycle index of the observation time range. The high-pass filtering can cut off the low
 206 frequency signals of turbulence to obtain the high frequency signals. An aliasing of
 207 half high frequency turbulence after the Fourier transformation is unavoidable. At this
 208 time, the correction for high frequency response will compensate for that loss. In
 209 order to acquire purely signals of different scale eddies in filtering processes, we take
 210 results of the band-pass filtering from $n=j$ to $n=N-j$ as required signals. This is referred
 211 to as j time filtering in this paper. Finally, the ergodicity of different scale eddies is
 212 analyzed using Eqs. (4)-(7).

213 **2.3 MOS of turbulent variance**

214 The characteristics of the relations of Monin-Obukhov Similarity (MOS) for the
 215 variance of different scale eddies are analyzed and compared to test feasibility of the
 216 MOS relation for ergodic and non-ergodic turbulence. In order to provide an
 217 experimental basis for utilizing MOST and developing the turbulence theory of ABL
 218 under the condition of the complex underlying surfaces, the problems of
 219 eddy-covariance technique of the turbulence observation in ASL are further explored
 220 on the basis of studying on the ergodicity and MOS relations of the variance of

221 different scale eddies.

222 The MOS relations of turbulent variance can be regarded as an effective
223 instrumentality to verify whether or not that the turbulent flow field is steady and
224 homogeneous (Foken et al. 2004). Under ideal conditions, the local MOS relations of
225 the variance of wind velocity, temperature and other factors can be expressed as
226 following:

$$227 \quad \sigma_i/u_* = \phi_i(z/L), \quad (i = u, v, w), \quad (10)$$

$$228 \quad \sigma_s/|s_*| = \phi_s(z/L), \quad (s = \theta, q). \quad (11)$$

229 where σ is turbulent variance; corner mark i is wind velocity u , v or w ; s stands for
230 scalar, such as potential temperature θ and humidity q ; u_* is friction velocity and

231 defined as $u_* = \left(\overline{u'w'^2} + \overline{v'w'^2} \right)^{1/4}$; s_* is turbulent characteristic quantity related to

232 scalar defined as $s_* = -\overline{w's'}/u_*$; and that M-O length L is defined as (Hill 1989):

$$233 \quad L = u_*^2 \theta / [\kappa g (\theta_* + 0.61 \theta q_* / \rho_d)], \quad (12)$$

234 where ρ_d is dry air density .

235 A large number of research results show that, in the case of unstable stratification,
236 $\phi_i(z/L)$ and $\phi_s(z/L)$ can be expressed in the following forms (Panofsky et al. 1977;
237 Padro 1993; Katul et al. 1999):

$$238 \quad \phi_i(z/L) = c_1 (1 - c_2 z/L)^{1/3}; \quad (13)$$

$$239 \quad \phi_s(z/L) = \alpha_s (1 - \beta_s z/L)^{-1/3}. \quad (14)$$

240 where c_1 , c_2 , α and β are coefficient to be determined by the field observation. In the
241 case of stable stratification, $\phi_s(z/L)$ approximates a constant and $\phi_i(z/L)$ is still the
242 1/3 function of z/L . The turbulent characteristics of eddies in different temporal and
243 spatial scale are analyzed and compared with the mean and autocorrelation ergodic
244 theorems, to test feasibility of MOS relations under the condition of the ergodic and
245 non-ergodic turbulence.

246 3 The sources and processing of data

247 In this study two turbulence data sets are used for completely different purposes. The
248 first turbulence data set is the data measured by the eddy-covariance technique under

249 the homogeneous surface in Nagqu Station of Plateau Climate and Environment
250 (NSPCE), Chinese Academy of Sciences (CAS). The data set in NSPCE/CAS
251 includes the data that are measured by 3-D sonic anemometer and thermometer
252 (CSAT3) with 10 Hz as well as infrared gas analyzer (Li7500) in ASL from 23 July to
253 13 September 2011. In addition, the second turbulence data set of CASES-99 (Poulos
254 et al. 2002; Chang and Huynh. 2002) is used to verify the ergodicity of turbulence
255 observed by multi-stations. CASES-99 has seven observation sites to be equivalent to
256 seven observation stations. The data in the central tower of CASES-99 include that
257 measured by sonic anemometer and thermometer (CSAT3) with 20 Hz and the
258 infrared gas analyzer (Li7500) at 10m on tower with 55 m height in ASL. The other
259 six sub-sites of CASES-99 surrounding the central tower, sn1, sn2 and sn3 are located
260 100 m away from the central tower, the sub-site sn4 is 280 m away, and sub-sites
261 sn5 and sn6 are located 300 m away. The data of sub-sites include that measured by
262 3-D sonic anemometer (ATI) and Li7500 at 10 m height on the towers. The analyzed
263 results with two data sets are compared each other to test universality of the research
264 results.

265 The geographic coordinate of NSPCE/CAS is 31.37°N, 91.90°E, and its altitude is
266 4509 m a.s.l. The observation station is built on flat and wide area except for a hill of
267 about 200 m at 2 km distance in the north, and floor area is 8000m². The ground
268 surface is mainly composed of sandy soil mixed with sparse fine stones, and a plateau
269 meadow with vegetation of 10-20 cm. The roughness length and displacement height
270 of underlying surface of NSPCE meadow are respectively 0.009 m and 0.03 m.
271 CASES-99 is located in prairie of Kansas US. The geographic coordinate of
272 CASES-99 central tower is 37.65°N, 96.74°W. The observation field is flat and
273 growth grasses about 20-50 cm during the observation period, while the roughness
274 length and displacement height of CASES-99 underlying surface are 0.012 m and
275 0.06 m, respectively (Martano 2000).

276 These data are used to study the ergodicity of turbulent eddies in ABL. Firstly the
277 inaccurate data caused by spike are deleted before data analyses. Subsequently, the
278 data are divided into continuous sections of 5-hour, and the signals of 1-hour are
279 obtained applying filtering of Eqs. (8) and (9) for each 5-hour data. In order to delete
280 further the abnormal inaccurate data, the data are divided once again into 12
281 continuous fragments of 5-min in 1-hour. The variances of velocity and temperature

282 are calculated and compared each other for the fragments. The data that deviation is
283 less than $\pm 15\%$ including an instrumental error about $\pm 5\%$ are selected to use.
284 Moreover, temperature of the ultrasonic pulse signals is converted to the absolute
285 temperature (Schotanus et al. 1983; Kaimal and Gaynor 1991). Then all data without
286 spike for 25 days are done the coordinate rotation using the plane fitting method to
287 improve the levelness of instrument installation (Wilczak 2001). The trend correction
288 (McMillen 1988; Moore 1986) is used to exclude the influence of low-frequency
289 trend effect caused by the diurnal variations and weather processes. The Webb
290 correction (Webb et al. 1980) is a component of surface energy balance in physical
291 nature, but not the component of turbulent eddy. However, this study is to analyze the
292 ergodicity of turbulent eddies. According to our preliminary analysis about the
293 ergodicity of turbulent eddies, such correction may cause the unreasonable deviation
294 from the prediction with Eq. (14). We thus do not perform the Webb correction in our
295 research on the ergodicity.

296 **4. Result analyses**

297 Applying the two data sets from NSPCE/CAS and CASES-99, the ergodicity of
298 different temporal scale eddies is tested. Here as an example, we select representative
299 data measured at level of 3.08m in NSPCE/CAS during three time frames, namely
300 3:00-4:00, 7:00-8:00 and 13:00-14:00 China Standard Time (CST) on 25 August in
301 clear weather to test and demonstrate the ergodicity of different temporal scale eddies.
302 These three time frames represent three situations, i.e. the nocturnal stable boundary
303 layer, early neutral boundary layer and midday convective boundary layer.

304 Eqs. (8) and (9) are used to perform band-pass filtering from $n=j$ to $n=N-j$ to
305 acquire the signals of eddies corresponding temporal scale including 2 min, 3 min, 5
306 min, 10 min, 30 min and 60 min. The turbulence characteristics and ergodicity of
307 eddies in the different temporal scale including 2 min, 3 min, 5 min, 10 min, 30 min
308 and 60 min are studied using above processed data for three time frames.

309 **4.1 M-O eddy local stability and M-O stratification stability**

310 The M-O stratification stability parameter z/L describes a whole characteristic of the
311 mechanical and buoyancy effect on the ASL turbulence. However this study will
312 decompose the turbulence into different scale eddies. Considering that the property of
313 different scale eddies of the atmospheric turbulence varies with the atmospheric
314 stability parameter z/L , a M-O eddy local stability that is limited in the certain scale

315 range of eddies is defined as z/L_c , so as to analyze relations between the stratification
316 stability and ergodicity of the different scale eddies for the wind velocity, temperature
317 and other factors. It is worth noting that the M-O eddy local stability, z/L_c , is different
318 from the M-O stratification stability, z/L .

319 As a typical example, the eddy local stabilities, z/L_c , of the different temporal scales
320 for the three time frames from the nighttime to the daytime are shown in Table 1. The
321 results show that the eddy local stability z/L_c below 2 min in temporal scale at time
322 3:00-4:00 AM(CST) during the nighttime time frame is 0.59, thus it is stable
323 stratification. But as the eddy temporal scale gradually increases from 3 min, 5 min
324 and 10 min to 60 min, the eddy local stability, z/L_c , gradually decreases to 0.31 and
325 0.28. Even starting from 10 min in the temporal scale, the eddy local stability
326 decreases from -0.01 to -0.07. It seems that the eddy local stability gradually varies
327 from stable to unstable as the eddy temporal scale increases. At 7:00-8:00 AM (CST)
328 during the morning time frame, the eddy local stability z/L_c from 2 min to 60 min in
329 the temporal scale eventually decreases from 0.52, 0.38, 0.16 and 0.15 to -0.43 in 30
330 min and a minimum of -1.29 in 60 min. It means that eddies in the temporal scales of
331 30 min and 60 min have high local instability. However, at 14:00-15:00 PM (CST)
332 during the midday time frame, eddies in the temporal scales from 2 min to 60 min are
333 all unstable. Now $-z/L_c$ is defined as eddy local instability. As the eddy scale increases,
334 the eddy local instability in the scales from 2 min to 3 min also increases. And that its
335 value reaches a maximum of 0.44 as the eddy scale is at 5 min. But as the eddy scale
336 increases continuously, the eddy local instability is reduced.

337 The M-O eddy local stability is not entirely the same as the M-O stratification
338 stability of ABL in the physical significance. The M-O stratification stability of ABL
339 indicates the overall effect of atmospheric stratification in the ABL on the stability
340 including all eddies in integral boundary layer. The M-O stratification stability z/L is
341 stable 0.02 at 3:00-4:00 AM (CST) for no filtering data to include whole turbulent
342 signals, but unstable -0.004 and -0.54 at 7:00-8:00 and 13:00-14:00 PM (CST),
343 respectively. However the eddy local stability is only a local effect of atmospheric
344 stratification on the stability of eddies in a certain scale. As the eddy scale increases,
345 the eddy local stability z/L_c will vary accordingly. The aforesaid results indicate that
346 the local stability of small-scale eddies is stable in the nocturnal stable boundary layer,
347 but it is possibly unstable for the large-scale eddies. As a result, a sink effect on the

348 small-scale eddies in the nocturnal stable boundary layer, but a positive buoyancy
349 effect on the large-scale eddies. However, in diurnal unstable boundary layer, the eddy
350 local instability of 3 min scale reaches a maximum, and then the instability gradually
351 decreases as the eddy scale increases. Therefore, eddies of 3 min scale hold maximum
352 buoyancy, but the eddy buoyancy decreases as the eddy scale increases continuously.
353 Nevertheless, the small-scale eddies are more stable than the large scale eddies in the
354 nocturnal stable boundary layer; the large-scale eddies are more stable than the small
355 scale eddies in the diurnal convective boundary layer with unstable stratification. The
356 above facts signify that it is common that there exist mainly the small-scale eddies in
357 the nocturnal boundary layer with stable stratification. And it is also common that
358 there exist mainly the large-scale eddies in the diurnal convective boundary layer with
359 unstable stratification. Therefore, it can well understand that the small-scale eddies are
360 dominant in the nocturnal stable boundary layer, while the large-scale eddies are
361 dominant in the diurnal convective boundary layer.

362 **4.2 Verification of mean ergodic theorem of eddies in different temporal scale**

363 In order to verify the mean ergodic theorem, we calculate the mean and
364 autocorrelation functions using Eq. (2) and Eq. (3), then calculate the variation of
365 mean ergodic function $Ero(A)$ using Eq. (5) of eddies in the different temporal scale
366 with relaxation time τ to be cut off with $\tau_{i=n}$. The mean ergodic functions, $Ero(A)$, of
367 vertical velocity, temperature and specific humidity of the different scale eddies are
368 calculated using data at level of 3.08m at 3:00-4:00, 7:00-8:00 and 13:00-14:00 (CST)
369 for three time frames in NSPCE/CAS, as shown in Figs. 1-3 respectively. Since the
370 ergodic function varies within a large range, the ergodic functions are normalized
371 according to the characteristic quantity of relevant variables ($A_* = \mathbf{u}_*, |\theta_*|, |q_*|$). That is
372 to say, functions in all following figures are the dimensionless ergodic functions,
373 $Ero(A)/A_*$.

374 Comprehensive analyses of the characteristics of mean ergodicity of atmospheric
375 turbulence as well as the relevant causes:

376 4.2.1 Verifying mean ergodic theorem of different scale eddies

377 According to the mean ergodic theorem, Eq. (4), the mean ergodic function $Ero(A)/A_*$
378 will converge to 0 if the time approaches infinite. This is only a theoretical result of
379 the stationary random processes. A practical mean ergodic function is calculated under
380 the condition of that relaxation time $\tau_{i=n}$ is cut off. If the mean ergodic function

381 $Ero(A)/A^*$ converges approximately to 0 in relaxation time $\tau_{i=n}$, it will be considered
382 that random variable A approximately satisfies the mean ergodic theorem. The mean
383 ergodic function deviates more from zero, the mean ergodicity will be of poor quality.
384 Consequently, we can judge approximately the mean ergodic theorem of different
385 scale eddies whether or not holds. Figs. 1-3 clearly show that, regardless of the
386 vertical velocity, temperature or humidity, the $Ero(A)/A^*$ of eddies below 10 min in the
387 temporal scale will swing around zero within a small range; thus we can conclude that
388 the mean ergodic function $Ero(A)/A^*$ of eddies below 10 min in the temporal scale
389 converges to zero to satisfy effectively the condition of mean ergodic theorem. For
390 eddies of 30 min and 60 min, which are larger scale, the mean ergodic function
391 $Ero(A)/A^*$ will deviate further from zero. In particular, the mean ergodic function
392 $Ero(A)/A^*$ of eddies of 30 min and 60 min for the temperature and humidity does not
393 converge, and even diverges. Above results show that the mean ergodic function of
394 eddies of 30 min and 60 min cannot converge to zero or cannot satisfy the condition
395 of mean ergodic theorem.

396 4.2.2 Comparison of the convergence of mean ergodic functions of vertical velocity, 397 temperature and humidity

398 As seen from the Figs. 1-3, dimensionless mean ergodic function of the vertical
399 velocity is compared with respective function of the temperature and humidity, it is
400 3-4 magnitudes less than those in the nocturnal stable boundary layer; 1-2 magnitudes
401 less than those in the early neutral boundary layer; and about 2 magnitudes less than
402 those in the midday convective boundary layer. For example, at 3:00-4:00 PM (CST)
403 during nighttime time frame, the dimensionless mean ergodic function of vertical
404 velocity is 10^{-5} in magnitude, while respective magnitudes of function value of the
405 temperature and humidity are 10^{-1} and 10^{-2} ; at 7:00-8:00 AM (CAT) during morning
406 time frame, magnitude of mean ergodic function of the vertical velocity is 10^{-4} , while
407 the respective magnitudes of function value of the temperature and humidity are 10^{-2}
408 and 10^{-3} ; at 13:00-14:00 PM(CST) during midday time frame, magnitude of mean
409 ergodic function of the vertical velocity is 10^{-4} , while the magnitudes of function
410 value of the temperature and humidity are both 10^{-2} . These results show that the
411 dimensionless mean ergodic function of vertical velocity converges to zero much
412 more easily than respective function value of the temperature and humidity, and that
413 the vertical velocity satisfies the condition of mean ergodic theorem to overmatch

414 more than the temperature and humidity.

415 4.2.3 Temporal scale and spatial scale of turbulent eddies

416 For wind velocity of $1-2 \text{ ms}^{-1}$, eddy spatial scale in the temporal scale 2 min is in the
417 range of 120-240 m, and eddy spatial scale in the temporal scale of 10 min is in the
418 range of 600-1200 m. The eddy spatial scale in the temporal scale of 2 min is
419 equivalent to ASL height, and the eddy spatial scale in the temporal scale of 10 min is
420 equivalent to ABL height. The eddy spatial scale within the temporal scales of 30-60
421 min is around 1800-3600 m, and this spatial scale clearly exceeds ABL height to
422 belong to scope of the atmospheric local circulation. According to the stationary
423 random processes definition (1) and mean ergodic theorem, the stationary random
424 processes must be smooth in relaxation time τ . The eddies below temporal scale of 10
425 min, i.e., below ABL height, can effectively satisfy the condition of mean ergodic
426 theorem, and must be the stationary random processes of mean ergodicity. However,
427 eddies in the temporal scales of 30 min and 60 min exceed ABL height and do not
428 satisfy the condition of mean ergodic theorem.

429 4.2.4 Turbulence ergodicity of all eddies in possible scales in ABL

430 To facilitate comparison, Fig. 4 shows the variation of mean ergodic function $Ero(A)$
431 of the vertical velocity (a), temperature (b) and specific humidity (c) before filtering
432 with relaxation time τ at 14:00-15:00 PM (CST) during midday time frame in
433 convective boundary layer. It is obvious that Fig. 4 is unfiltered mean ergodic
434 function of eddies in all possible scales in ABL. The Fig. 4 compares with Figs. 1c, 2c
435 and 3c, which are the mean ergodic function $Ero(A)/A^*$ of vertical velocity,
436 temperature and humidity after filtering at 14:00-15:00 PM (CST) during the midday
437 time frame. The result shows that the mean ergodic functions before filtering are
438 greater than that after filtering. As shown in Figs. 1c, 2c and 3c, the magnitude for the
439 vertical velocity is 10^{-4} and the magnitudes for the temperature and specific humidity
440 are both 10^{-2} . According to Fig. 4, the magnitude of vertical velocity $Ero(A)/A^*$ is 10^{-3}
441 and the magnitudes of temperature and specific humidity are both 10^0 , therefore 1-2
442 magnitudes are almost decreased after filtering. Moreover, all trend upward deviating
443 from zero for vertical velocity and temperature, but downward deviating from zero for
444 specific humidity. It is thus clear that, at 14:00-15:00 PM (CST) during the midday
445 time frame, when is equivalent to the local time 12:00-13:00, the unfiltered mean
446 ergodic function of eddies in all possible scales in convective boundary layer cannot

447 converge to zero before filtering, i.e., cannot satisfy the condition of mean ergodic
448 theorem. This may be that eddies in all possible scales before filtering include the
449 local circulation in convective boundary layer. So we argue that, under general
450 situations, the eddies only below 10 min in the temporal scale or within 600-1200 m
451 in the spatial scale in ABL must be the stationary random processes of mean
452 ergodicity.

453 4.2.5 Relation between the ergodicity and local stability of different scale eddies

454 Table 1 list the corresponding relation of eddy local stabilities z/L_c of eddies of
455 different scales with the different time frames. It shows that the eddy local stabilities
456 z/L_c of different scale eddies are different, due to the fact that the temperature
457 stratification in ABL has different effect on the stability for different scale eddies.
458 Even entirely contrary results can occur. At the same time, the stratification that
459 causes the large scale eddy to ascend with buoyancy may cause the small scale eddy
460 to descend. However, the results in Figs. 1-3 show that the ergodicity is mainly related
461 to the eddy scale, and its relation with the atmospheric temperature stratification
462 seems secondary.

463 **4.3 Verification of autocorrelation ergodic theorem for different scale eddies**

464 In this section, Eqs. (7a) and (7b) are used to verify the autocorrelation ergodic
465 theorem. It is accordant with Sect. 4.2 that the turbulent eddies below 10 min in
466 temporal scale satisfy the mean ergodic condition in the various time frames, i.e., the
467 turbulent eddies below 10 min in temporal scale are at least strictly stationary random
468 processes or narrow stationary random processes whether in the nocturnal stable
469 boundary layer, or in the early neutral boundary layer and midday convective
470 boundary layer. Then we analyze further the different scale eddies that satisfy the
471 mean ergodic condition whether or not also satisfy the autocorrelation ergodic
472 condition, so as to verify atmospheric turbulence is whether narrow or wide stationary
473 random processes. The autocorrelation ergodic function of turbulence variable A
474 under the condition of truncated relaxation time $\tau_{i=n}$ is calculated according to Eq. (7a)
475 to determine the variation of autocorrelation ergodic function $Er(A)$ with relaxation
476 time τ . As with the mean ergodic function $Ero(A)$, if the autocorrelation ergodic
477 function $Er(A)$ of eddies of 2 min, 3 min, 5 min, 10 min, 30 min and 60 min in the
478 temporal scale within the relaxation time $\tau_{i=n}$ approximates 0, then A shall be deemed
479 to be approximately ergodic; the more the autocorrelation ergodic function deviates

480 from 0, the worse the autocorrelation ergodicity becomes. Therefore, this method can
481 be used to judge approximately whether the different scale eddies satisfy the
482 condition of autocorrelation ergodic theorem.

483 As an example for the vertical velocity, Fig. 5 shows the variation of normalized
484 autocorrelation ergodic function $Ero(w)/u^*$ of the turbulent eddies of 2 min, 3 min, 5
485 min, 10 min, 30 min and 60 min in the temporal scale with relaxation time τ at
486 3:00-4:00, 7:00-8:00 and 13:00-14:00 (CST) during the time frames respectively.
487 Some basic conclusions are drawn from Fig. 5 as following:

- 488 1. After comparing the Figs. 5a-c with the Figs. 1a-c, i.e., comparing the
489 dimensionless mean ergodic function $Ero(w)/u^*$ of vertical velocity with the
490 dimensionless autocorrelation ergodic function $Er(w)/u^*$, two basic characteristics
491 are very clear. First, the magnitudes of the dimensionless autocorrelation ergodic
492 function $Er(w)/u^*$, regardless of whether in the nocturnal stable boundary layer,
493 early neutral boundary layer or midday convective boundary layer, are all greatly
494 reduced. In Figs. 1a-c, the magnitudes of $Ero(w)/u^*$ are respectively 10^{-5} , 10^{-4} and
495 10^{-4} , and the magnitudes of $Er(w)/u^*$ are respectively 10^{-7} , 10^{-5} and 10^{-5} as shown in
496 Figs. 5a-c. The magnitudes of $Er(w)/u^*$ reduce by 1-2 magnitudes compared with
497 those of $Ero(w)/u^*$. Second, all autocorrelation ergodic functions $Er(w)/u^*$ of the
498 eddies of 30 min and 60 min in temporal scale, regardless of whether they are in
499 the stable boundary layer, natural boundary layer or convective boundary layer, are
500 all reduced and approximate to $Ero(w)/u^*$ of the eddies below 10 min in temporal
501 scale.
- 502 2. The above two basic characteristics imply that the autocorrelation ergodic function
503 $Er(w)/u^*$ of the stable boundary layer, neutral boundary layer or convective
504 boundary layer converges to 0 faster than the mean ergodic function $Ero(w)/u^*$; the
505 autocorrelation ergodic function of eddies of 30 min and 60 min in temporal scale
506 also converges to 0 and satisfies the condition of autocorrelation ergodic theorem,
507 except for the fact that the autocorrelation ergodic function $Er(w)/u^*$ of the eddies
508 below 10 min in temporal scale can converge to 0 and satisfy the condition of
509 autocorrelation ergodic theorem.
- 510 3. According to the autocorrelation ergodic function Eq. (7a), the eddies of 30 min, 60
511 min and below 10 min in the temporal scale, regardless of whether they are in the
512 stable boundary layer, neutral boundary layer or convective boundary layer, all

513 eddies satisfy the condition of autocorrelation ergodic theorem. Therefore, in
514 general ABL turbulence is the stationary random processes of autocorrelation
515 ergodicity.

516 4. The above results show that the eddies below 10 min in temporal scale in the
517 nocturnal stable boundary layer, early neutral boundary layer and midday
518 convective boundary layer not only satisfy the condition of mean ergodic theorem,
519 but also they satisfy the condition of autocorrelation ergodic theorem. Therefore,
520 eddies below 10 min in the temporal scale are a wide ergodic stationary random
521 processes. Although the eddies of 30 min and 60 min in temporal scale in the stable
522 boundary layer, neutral boundary layer and convective boundary layer satisfy the
523 condition of autocorrelation ergodic theorem, but they dissatisfy the condition of
524 mean ergodic theorem. Therefore, eddies of 30 min and 60 min in the temporal
525 scale are neither narrow ergodic stationary random processes, nor wide ergodic
526 stationary random processes.

527 **4.4 Ergodic theorem verification of different scale eddies for the multi-stations**

528 The basic principle of turbulence average is an ensemble average of the space, time
529 and state. Sections 4.2 and 4.3 verify the mean ergodic theorem and autocorrelation
530 ergodic theorem of atmospheric turbulence using field observational data, so that the
531 finite time average of a single station can be used to substitute for the ensemble
532 average for the ergodic turbulence. This section examines the ergodicity of different
533 scale eddies using the observational data of center tower and six sub-sites of
534 CASES-99, in all seven sites to be equivalent to seven stations. When the data are
535 selected, it is considered that if the eddies are not evenly distributed at the seven sites,
536 then the observation results at the seven sites may have originated from many eddies
537 in the large scale. For this reason, the high frequency variance spectrum in excess of
538 0.1 Hz is compared firstly. Based on the observational error, if the scatter of all high
539 frequency variances does not exceed the average by $\pm 10\%$, then it is assumed that the
540 turbulence is evenly distributed at the seven observation sites. And then, 17 datasets
541 are chosen from among the observed turbulence data from 5 to 30 October, and these
542 data sets represent typical strong turbulence at noon on the sunny day. As an example,
543 the same method as described in Sections 4.2 and 4.3 is used to respectively calculate
544 variation of the mean ergodic function and autocorrelation ergodic function with
545 relaxation time τ for the vertical velocity at 10:00-11:00 AM on 7 October. The time

546 series composed of the above data sets is performed band-pass filtering in 2 min, 3
547 min, 5 min, 10 min, 30 min and 60 min. The variations of mean ergodic function
548 $Ero(w)/u^*$ and autocorrelation ergodic function $Er(w)/u^*$ with relaxation time τ are
549 analyzed for the vertical velocity to test the ergodicity of different scale eddies for
550 observation of the multi-stations. Fig. 6a shows variation of mean ergodic function
551 $Ero(w)/u^*$ with the relaxation time τ for the vertical velocity, and Fig. 6b shows
552 variation of autocorrelation ergodic function $Er(w)/u^*$ with the relaxation time τ .

553 The results show ergodic characteristics of different scale eddies measured with the
554 multi-stations as following:

555 Fig. 6a shows that the mean ergodic function of eddies below 30 min in temporal
556 scale converges to 0 very well, except for the fact that the mean ergodic function of
557 eddies of 60 min in temporal scale clearly deviates upward from 0. Fig. 6b shows that
558 autocorrelation ergodic function of all different scale eddies including 60 min in
559 temporal scale, gradually converges to 0. Therefore, eddies below 30 min in temporal
560 scale measured with the multi-stations satisfy the conditions of both the mean and
561 autocorrelation ergodic theorem, while eddies of 60 min in temporal scale only
562 satisfies the condition of autocorrelation ergodic theorem, but dissatisfy the condition
563 of mean ergodic theorem. These facts demonstrate that eddies below 30 min in
564 temporal scale are the wide ergodic stationary random processes for time series of
565 above data sets composed by the seven stations. This signifies that comparing of data
566 composed of the multi-stations with data from a single station, the eddy temporal
567 scale of wide ergodic stationary random processes is extended from below 10 min to
568 30 min. As analyzed above, if the eddies below 10 min in temporal scale are deemed
569 to be the turbulent eddies in the ABL with height about 1000 m, and the eddies of 30
570 min in the temporal scale, which is equivalent to that the space scale is greater than
571 2000 m, are deemed including eddy components of the local circulation in ABL, in
572 that way the multiple station observations can completely capture the local circulated
573 eddies, which space scale is greater than 2000 m.

574 **4.5 Average time problem of turbulent quantity averaging**

575 The atmospheric observations are impossible to repeat experiments exactly, must use
576 the ergodic hypothesis and replace ensemble averages with time averages. It arises a
577 problem how does determine the averaging time.

578 The analyses on the ergodicity of different scale eddies in above two sections

579 demonstrate that the eddies below 10 min in temporal scale as relaxation time $\tau=30$
580 min in the stable boundary layer, neutral boundary layer and convective boundary
581 layer not only satisfy the mean ergodic theorem, but also satisfy the autocorrelation
582 ergodic theorem. That is to say, they are namely wide ergodic stationary random
583 processes. Therefore, a finite time average of 30 min within relaxation time τ can be
584 used for substituting for the ensemble average to calculate mean random variable, Eq.
585 (2). However, the eddies of 30 min and 60 min in temporal scale in the stable
586 boundary layer and neutral boundary layer are only autocorrelation ergodic random
587 processes, neither narrow nor wide sense random processes. Therefore, when the
588 finite time average of 30 min can be used for substituting for the ensemble average to
589 calculate mean random variable Eq. (2), it may capture the eddies below 10 min in
590 temporal scale in stationary random processes, but cannot completely capture the
591 eddies in excess of 30 min in temporal scale. The above results signify that the
592 turbulence average is restricted not only by the mean ergodic theorem, but also is
593 closely related to the scale of turbulent eddies. In the atmospheric observations
594 performed using the eddy-covariance technique, the substitution of ensemble average
595 with finite time average of 30 min inevitably results in a high level of error, due to
596 loss of low frequency component information associating with the large-scale eddies.
597 However, although eddies of 30 min and 60 min in temporal scale in convective
598 boundary layer are not wide ergodic stationary random processes, they are
599 autocorrelation ergodic random processes. This may imply that the mean of
600 atmospheric turbulence in the convective boundary layer, which is calculated to
601 substitute the finite time average for the ensemble average, is often superior to the
602 results of the stable boundary layer and neutral boundary layer. Withal, the results in
603 the previous sections also show that the mean ergodic function of vertical velocity
604 may more easily converge to 0 than functions corresponding to the temperature and
605 humidity, i.e., the vertical velocity may more easily satisfy the condition of mean
606 ergodic theorem than the temperature and humidity. Therefore, in the observation
607 performed using the eddy-covariance technique, the result of vertical velocity is often
608 superior to those of the temperature and humidity. In the previous section, the results
609 also point out that multi-stations observation can completely capture eddy of the local
610 circumfluence in the ABL. Therefore, the multi-stations observation is more likely to
611 satisfy the ergodic assumption, and its results are much closer to the true values. In

612 order to determine the averaging time, Oncley (1996) defined an Ogive function of
613 cumulative integral

$$614 \quad Og_{x,y}(f_0) = \int_{\infty}^{f_0} Co_{x,y}(f) df \quad (15)$$

615 where x and y are any two variables, and their covariance is \overline{xy} , $Co_{xy}(f)$ is the
616 cospectrum of xy . If the Ogive function converges to a constant value at a frequency
617 $f=f_0$, this frequency could be converted to an averaging time. Ogive function of $\overline{u'w'}$
618 is often used to examine the minimal averaging time. As a comparison, here the
619 variation of Ogive functions of $\overline{w'^2}$ and $\overline{u'w'}$ with frequency at the height 3.08 m in
620 NSPCE/CAS for the three time frames is shown in Fig.7. The Fig.7 shows
621 convergence frequency of Ogive function for $\overline{w'^2}$ in the nighttime stable boundary
622 layer, morningtide neutral boundary layer and midday convection boundary layer is
623 respectively about at 0.01 Hz, 0.0001 Hz and 0.001 Hz. It is equivalent to the
624 averaging times about 2 min, 160 min and 16 min. For $\overline{u'w'}$, it converges about at
625 0.001 Hz only in the midday convection boundary layer to be equivalent to the
626 averaging time about 16 min; it seems no convergence in the nighttime stable and
627 morningtide neutral boundary layer. It is implied determining the averaging time
628 encounters a bit difficult with the Ogive function in the stable and neutral boundary
629 layer. Fig.7 shows also that when the frequency is lower than 0.0001Hz, Ogive
630 functions $\overline{u'w'}$ ascend in the stable boundary layer, but descend in the morningtide
631 neutral boundary layer and midday convection boundary layer. We must especially
632 note that Ogive function is a cumulative integral. So as Ogive function changes
633 direction from ascending to descending, it implies a possibility that there exists a
634 superimposing of the negative and positive momentum fluxes caused by a cross local
635 circulation effect in nighttime and midday. This cross local circulation in ABL may
636 cause the low frequency effect on the Ogive function. So that the local circulation in
637 ABL may be an important cause that Ogive fails to judge the averaging time. In this
638 work, the choice of averaging time with the ergodic theory seems superior to with the
639 Ogive function.

640 **4.6 MOS of turbulent eddies in different scales and its relation with ergodicity**

641 Turbulent variance is a most basic characteristic quantity of the turbulence.

642 Turbulence velocity variance, which represents turbulence intensity, and the variance

643 of scalars, such as temperature and humidity, effectively describes the structural
 644 characteristics of turbulence. In order to test MOS relation of the different scale
 645 eddies with ergodicity, the vertical velocity and temperature data of NSPCE/CAS
 646 from 23 July to 13 September are used to determine the MOS relationship of
 647 variances of vertical velocity and temperature for the different scale eddies, and to
 648 analyze its relation with the ergodicity.

649 The MOS relation of vertical velocity variance as following:

$$650 \quad \phi_i(z/L) = c_1(1 - c_2 z/L)^{1/3}, \quad z/L < 0, \quad (16)$$

$$651 \quad \phi_i(z/L) = c_1(1 + c_2 z/L)^{1/3}, \quad z/L > 0. \quad (17)$$

652 Fig. 8 and 9 respectively shows the MOS relation curves of different scale eddies for
 653 the vertical velocity and temperature variances in NSPCE/CAS. The figures (a), (b)
 654 and (c) of Fig. 8 and 9 are respectively the similarity curve of eddies of 10 min, 30
 655 min and 60 min in the temporal scale. Table 2 shows the relevant parameters of fitting
 656 curve of MOS relation for the vertical velocity variance. The correlation coefficient
 657 and residual of fitting curve are respectively expressed with R and S .

658 Fig. 8 and Table 2 show that the parameters of fitting curve are greatly different,
 659 even if the fitting curve modality of MOS relation of the vertical velocity variance is
 660 the same for the eddies in different temporal scales. The correlation coefficients of
 661 MOS fitting curve of the vertical velocity variance under the unstable stratification are
 662 large, but the correlation coefficients under the stable stratification are small. Under
 663 unstable stratification, the correlation coefficient of eddies of 10 min in the temporal
 664 scale reaches 0.97, while the residual is only 0.16; under the stable stratification, the
 665 correlation coefficient reduces to 0.76, and the residual increases to 0.25. With the
 666 increase of eddy temporal scale from 10 min (Fig. 8a) to 30 min (Fig. 8b) and 60 min
 667 (Fig. 8c), the correlation coefficients of MOS relation of the vertical velocity variance
 668 gradually reduce, and the residuals increase. The correlation coefficient in 60 min
 669 reaches a minimum; it is 0.83 under the unstable stratification, and only 0.30 under
 670 the stable stratification.

671 The temperature variance is shown in Fig. 9. MOS function to fit from eddies of 10
 672 min in the temporal scale under the unstable stratification is following:

$$673 \quad \phi_\theta(z/L_c) = 4.9(1 - 79.7 z/L_c)^{-1/3}. \quad (18)$$

674 As shown in Fig. 9a, the correlation coefficient of fitting curve is 0.91 and residual is

675 0.38. With increase of the eddy temporal scale, discreteness of MOS relation of the
676 temperature variance is enlarged quickly to incur that the appropriate curve cannot be
677 fitted.

678 The above results show that the discreteness of fitting curve of MOS relation for
679 the turbulence variance is enlarged with the increase of eddy temporal scale, whether
680 it is the vertical velocity or temperature. The points of data during the stationary
681 processes basically gather nearby the fitting curve of variance similarity relation,
682 while all data points during the non-stationary processes deviate significantly from the
683 fitting curve. However, the similarity of vertical velocity variance is superior to that of
684 the temperature variance. These results are consistent to the conclusions of ergodicity
685 test for the different scale eddies described in Sections 4.2-4.4. The ergodicity of the
686 small-scale eddies is superior to that of the larger-scale eddies, and eddies of 10 min
687 in the temporal scale have the best variance similarity relations. These results also
688 signify that when eddies in the stationary random processes satisfy the ergodic
689 condition, both the vertical velocity variance and temperature variance of eddies in the
690 different temporal scales comply with MOST very well; but, as for eddies with poor
691 ergodicity during non-stationary random processes, the variances deviate from MOS
692 relations.

693

694 **5 Discussions**

- 695 1. Galanti and Tsinober (2004) proved that the turbulence, which is temporally steady
696 and spatially homogeneous, is ergodic, but '*partially turbulent flows*' such as the
697 mixed layer, wake flow, jet flow, flow around and boundary layer flow may be
698 non-ergodic turbulence. However, it has been proven through atmospheric
699 observational data that the turbulence ergodicity is related to the scale of turbulent
700 eddies. Since the large-scale eddies in ABL may be strongly influenced by the
701 boundary disturbance, thus belong to 'partial turbulence'; however, since the
702 small-scale eddies in atmospheric turbulence may be not influenced by boundary
703 disturbance, may be temporally steady and spatially homogeneous turbulence. So
704 that the mean ergodic theorem and autocorrelation ergodic theorem are applicative
705 for turbulence eddies in the small scale in ABL, but the ergodic theorems aren't
706 applicative for the large-scale eddies, i.e., the small-scale eddies in the ABL are
707 ergodic and the large-scale eddies exceeding the ABL scale are non-ergodic.
- 708 2. The eddy-covariance technique for turbulence measurement is based on the ergodic

709 assumption. A lack of ergodicity related to the presence of large-scale eddy
710 transport can lead to a consider error of the flux measurement. This has already
711 been pointed out by Mauder et al. (2007) or Foken et al. (2011). Therefore, we
712 realize from the above results that the large scale eddies that exceed ABL height
713 may include component of non-ergodic random processes. The eddy-covariance
714 technique cannot capture the signals of large-scale eddies exceeded ABL scale to
715 result in the large error in the measurements of atmospheric turbulent variance and
716 covariance. MOST is developed under the condition of the steady time and
717 homogeneous surface. MOST conditions, steady time and homogeneous
718 underlying surface, are in line with the ergodic conditions, therefore the turbulence
719 variances, even the turbulent fluxes of eddies in different temporal scales may
720 comply with MOST very well, if the ergodic conditions of stationary random
721 processes are more effectively satisfied.

722 3. According to Kaimal and Wyngaard (1990), the atmospheric turbulence theory and
723 observation method were feasible and led to success under ideal conditions
724 including a short period, steady state and homogeneous underlying surface, and
725 through observation in the 1950s-1970s, but these conditions are rare in reality. In
726 the land surface processes and ecosystem, the turbulent flux observations in ASL
727 turn into a scientific issue, in which commonly interest researchers in the fields of
728 atmospheric sciences, ecology, geography sciences, etc. These observations must
729 be implemented under conditions such as with complex terrain, heterogeneous
730 surface, long period and unsteady state. It is necessary that more neoteric
731 observational tools and theories will be applied with new perspectives in future
732 research.

733 4. It is successful that the ergodic theorem of stationary random processes is
734 introduced from the mathematics into atmospheric sciences. It undoubtedly
735 provides a profited tool for overcoming the challenges encountering in the modern
736 measurements of atmospheric turbulent flow. At least it offers a promising first step
737 to diagnosticate directly the ergodic hypotheses for ASL flows as a criterion. And
738 that the necessary and sufficient condition of ergodic theorem can use to judge the
739 applicative scope of eddy-covariance technique and MOST, and seek potential
740 disable reasons for using them in the ABL.

741 5. In the future, we shall keep up to study the ergodic problems for the atmospheric

742 turbulence measurements under the conditions of complex terrain, heterogeneous
743 surface and unsteady, long observational period, and to seek effective schemes. The
744 above results indicate the atmospheric turbulent eddies below the scale of ABL can
745 be captured by the eddy-covariance technique and comply with MOST very well.
746 Perhaps MOST can be as the first order approximation to deal with the turbulence
747 of eddies below ABL scale satisfying the ergodic theorems, then to compensate the
748 effects of eddies dissatisfying the ergodic theorem, which may be caused by the
749 advection, local circulation, low frequency effect, etc. under the complex terrain,
750 heterogeneous surface. For example, we developed a turbulent theory of
751 non-equilibrium thermodynamics (Hu, Y., 2007; Hu, Y., et al., 2009) to find the
752 coupling effects of vertical velocity, which is caused by the advection, local
753 circulation, and low frequency, on the vertical fluxes. The coupling effects of
754 vertical velocity may be as a scheme to compensate the effects of eddies
755 dissatisfying the ergodic theorems (Hu, Y., 2003; Chen, J., et al., 2007, 2013).

756 6. It is clear that such studies are preliminary, and many problems require further
757 research, and the attestation of more field experiments is necessary.

758

759 **6 Conclusions**

760 From the above results, we can draw the below preliminary conclusions:

- 761 1. The turbulence in ABL is an eddy structure. When the temporal scale of turbulent
762 eddies in ABL is about 2 min, the corresponding spatial scale is about 120-240 m
763 to be equivalent to ASL height; when the temporal scale of turbulent eddies in ABL
764 is about 10 min, the corresponding spatial scale is about 600-1200 m to be
765 equivalent to the ABL height. For the eddies of larger temporal and spatial scale,
766 such as eddies of 30-60 min in the temporal scale, the corresponding spatial scale
767 is about 1800-3600 m to exceed the ABL height.
- 768 2. The above results show that the ergodicity of atmospheric turbulence in ABL is not
769 only relative to the atmospheric stratification but also to the eddy scale of
770 atmospheric turbulence. For the atmospheric turbulent eddies below the ABL scale,
771 i.e. the eddies below about 1000 m in the spatial scale and about 10 min in the
772 temporal scale, the mean ergodic function $Ero(A)$ and autocorrelation ergodic
773 function $Er(A)$ converge to 0, i.e., they satisfy the conditions of mean and
774 autocorrelation ergodic theorem. However, for the atmospheric turbulent eddies

775 in excess of 2000-3000m in the spatial scale and in excess of 30-60 min in the
776 temporal scale, the mean ergodic function doesn't converge to 0, thus dissatisfy the
777 condition of mean ergodic theorem. Therefore, the turbulent eddies that is below
778 the ABL scale belong to the wide ergodic stationary random processes, but the
779 turbulent eddies that are larger than ABL scale belong to the non-ergodic random
780 processes, or even the non-stationary random processes.

781 3. Due to above facts, when the stationary random process information of eddies
782 below 10 min in the temporal scale and below 1000 m of ABL height in the spatial
783 scale can be captured, the atmospheric turbulence may satisfy the condition of
784 mean ergodic theorem. Therefore, an average of finite time can be used to
785 substitute for the ensemble average to calculate the mean of random variable as
786 measuring atmospheric turbulence with the eddy-covariance technique. But for the
787 turbulence of eddies to be larger than 30 min in temporal scale, i.e., 2000 m in
788 spatial scale magnitude, it dissatisfy the condition of mean ergodic theorem, so that
789 the eddy-covariance technique cannot completely capture the information of
790 non-stationary random processes. This will inevitably cause a high level of error
791 when the average of finite time is used to substitute for the ensemble average in the
792 experiments due to the loss of low frequency component information associating
793 with the large-scale eddies.

794 4. Although the atmospheric temperature stratification has different effects on the
795 stability of eddies in the different scales, the ergodicity is mainly related to the
796 eddy local stability, and its relation with the stratification stability of ABL is
797 secondary.

798 5. The data series composed from seven stations compare with the observational data
799 from a single station. The results show that the temporal and spatial scale of eddies
800 to belong to the wide ergodic stationary random processes are extended from 10
801 min to below 30 min and from 1000 m to below 2000 m respectively. This signifies
802 that the ergodic assumption is more likely to be satisfied well with multi-stations
803 observation, and observational results produced by the eddy-covariance technique
804 are much closer to the true values when calculating the turbulence averages,
805 variances or fluxes.

806 6. If the ergodic conditions of stationary random processes are more effectively
807 satisfied, then the turbulence variances of eddies in the different temporal scale

808 can comply with MOST very well; however, the turbulence variances of the
809 non-ergodic random processes deviate from MOS relations.

810

811 *Acknowledgements.* This study is supported by Project Granted Nos. 91025011,
812 91437103 of the National Natural Science Foundation of China and Project Granted
813 No. 2010CB951701-2 of the National Program on Key Basic Research. This work
814 was strongly supported by Heihe Upstream Watershed Ecology-Hydrology
815 Experimental Research Station, Chinese Academy of Sciences. We would like to
816 express my sincere regards for their support. And that we thank Dr. Gordon Maclean
817 in NCAR for providing the detailed data of CASES-99 used in this study, and thank
818 referees and editor very much for heartfelt comments, discussions and marked errors.

819

820 References

821 Aubinet, M., Vesala, T., and Papale, D.: Eddy covariance, a practical guide to
822 measurement and data analysis, Springer, Dordrecht, Heidelberg, London, New
823 York, 438, 2012.

824 Birkhoff, G. D.: Proof of the ergodic theorem, Proc. Nat. Acad. Sci. USA. 18,
825 656-660, 1931.

826 Boltzmann, L.: Analytischer beweis des zweiten Hauptsatzes der mechanischen
827 Wärmetheorie aus den Sätzen über das Gleichgewicht der lebendigen Kraft, Wiener
828 Berichte , 63, 712-732, in WAI, paper 20, 1871.

829 Chang, S. S. and Huynh, G. D.: Analysis of sonic anemometer data from the
830 CASES-99 field experiment. Army Research Laboratory, Adelphi, MD. 2002.

831 Chen, J., Hu Y., and Zhang L.: Principle of cross coupling between vertical heat
832 turbulent transport and vertical velocity and determination of cross coupling
833 coefficient, Adv. Atmos. Sci., 23 (4), 639-648, 2007.

834 Chen, J., Hu, Y., Lu, S., and Yu, Ye.: Experimental demonstration of the coupling
835 effect of vertical velocity on latent heat flux, Sci. China. Ser. D-Earth Sci., 56,

836 1-9, 2013.

837 Eichinger, W. E., Parlange, M. B., Katul, G. G.: Lidar measurements of the
838 dimensionless humidity gradient in the unstable ASL, Lakshmi, V., Albertson, J.
839 and Schaake, J., Koster, R. D., Duan, Q., Land Surface Hydrology, Meteorology,
840 and Climate, American Geophysical Union, Washington, D. C. 7-13, 2001.

841 Ehrenfest, P. and T. Ehrenfest-Afanassjewa (1912), The Conceptual Foundations of
842 the Statistical Approach in Mechanics , New York: Cornell University Press,
843 1959.

844 Foken, T., Wichura, B.: Tools for quality assessment of surface-based flux
845 measurements. *Agric For Meteorol.*, 78, 83-105, 1996.

846 Foken, T., Göckede, M., Mauder, M., Mahrt, L., Amiro, B. D., and Munger, J. W.:
847 Post-field data quality control, in: Handbook of micrometeorology: a guide for
848 surface flux measurement and analysis, Lee, X., Massman, W. J., and Law, B.:
849 Kluwer, Dordrecht, 181-208, 2004.

850 Foken, T., Aubinet, M., Finnigan, J. J., Leclerc, M. Y., Mauder, M., Paw, U. K. T.:
851 Results of a panel discussion about the energy balance closure correction for
852 trace gases. *Bull Am. Meteorol. Soc.*, 92, ES13-ES18, 2011.

853 Galanti, B. and Tsinober, A.: Is turbulence ergodic? *Phys. Lett. A*, 330, 173–18, 2004.

854 Higgins, C. W., Katul, G. G., Froidevaux, M., Simeonov, V. and Parlange, M. B.:
855 Atmospheric surface layer flows ergodic? *Geophys. Res. Lett.*, 40, 3342-3346,
856 2013.

857 Hill, R. J.: Implications of Monin–Obukhov similarity theory for scalar quantities, *J.*
858 *Atmos. Sci.* 46, 2236–2244, 1989.

859 Hu, Y.: Convergence movement influence on the turbulent transportation in
860 atmospheric boundary layer, *Adv. Atmos. Sci.*, **20**, 794-798, 2003.

861 Hu, Y., Chen, J., Zuo, H.: Theorem of turbulent intensity and macroscopic mechanism
862 of the turbulence development, *Sci China Ser D-Earth Sci*, **37**, 789-800, 2007.

863 Hu, Y., and Chen, J.: Nonequilibrium Thermodynamic Theory of Atmospheric
864 Turbulence, In: *Atmospheric Turbulence, Meteorological Modeling and*
865 *Aerodynamics*, Edited by Lang P. R. and Lombargo F. S., Nova Science
866 Publishers, New York., 59-110, 2010.

867 Kaimal, J. C. and Wyngaard, J. C.: The Kansas and Minnesota experiments, *Bound.*
868 *Lay. Meteor.*, 50, 31-47, 1990.

869 Kaimal, J. C. and Gaynor, J. E.: Another look at sonic thermometry, *Bound. Lay.*
870 *Meteor.*, 56, 401–410, 1991.

871 Katul, G. G., Hsieh, C. I.: A note on the flux-variance similarity relationships for heat
872 and water vapor in the unstable atmospheric surface layer, *Bound. Lay. Meteor.*, 90,
873 327–338, 1999.

874 Katul, G., Cava, D., Poggi, D., Albertson, J., and Mahrt, L.: Stationarity, homogeneity,
875 and ergodicity in canopy turbulence, in: *Handbook of micrometeorology: a guide*
876 *for surface flux measurement and analysis*, Lee, X., Massman, W., and Law, B.,
877 Kluwer Academic Publishers, Dordrecht/BOSTON/LONDON , 161–180, 2004.

878 Krengel, U.: *Ergodic theorems*, de Gruyter, Berlin, New York, 363, 1985.

879 Lennaert van, V., Shigeo, K., and Genta, K.: Periodic motion representing isotropic
880 turbulence, *Fluid Dyn. Res.*, 38, 19–46, 2006.

881 Li, X., Hu, F., Pu, Y., Al-Jiboori, M. H., Hu, Z., and Hong, Z.: Identification of
882 coherent structures of turbulence at the atmospheric surface layer, *Adv. Atmos.*
883 *Sci.*, 19(4), 687-698, 2002.

884 Martano, P.: Estimation of surface roughness length and displacement height from
885 single-level sonic anemometer data, *J. Appl. Meteorol.*, 39(5), 708–715, 2000.

886 Mattingly, J. C.: On recent progress for the stochastic Navier Stokes equations,
887 Journées équations aux dérivées partielles, Univ. Nantes, Nantes, Exp. No. XI,
888 1-52, 2003.

889 Mauder, M., Desjardins, R. L., MacPherson, J.: Scale analysis of airborne flux
890 measurements over heterogeneous terrain in a boreal ecosystem. *J. Geophys. Res.*
891 112, D13, 2007.

892 McMillen, R. T.: An eddy correlation technique with extended applicability to non
893 simple terrain, *Bound. Lay. Meteor.*, 43, 231-245, 1988.

894 Moore, C. J.: Frequency response corrections for eddy correlation systems, *Bound.*
895 *Lay. Meteor.*, 37, 17-35, 1986.

896 Neumann, J. V.: Proof of the quasi-ergodic hypothesis, *Mathematics Proc. N. A. S.*,
897 18, 70-82, 1932.

898 Oncley, S. P., Friehe, C. A., Larue, J. C., Businger, J. A., Itsweire, E. C., Chang, S. S.:
899 Surface-Layer Fluxes, Profiles, and Turbulence Measurements over Uniform
900 Terrain under Near-Neutral Conditions, *J. Atmos. Sci.*, 53 (7), 1029-1044, 1996.

901 Padro, J.: An investigation of flux-variance methods and universal functions applied
902 to three land-use types in unstable conditions, *Bound. Lay. Meteor.*, 66, 413-425,
903 1993.

904 Panofsky, H. A., Lenschow, D. H., and Wyngaard, J. C.: The characteristics of
905 turbulent velocity components in the surface layer under unstable conditions. *Bound.*
906 *Lay. Meteor.*, 11, 355-361, 1977.

907 Papoulis, A. and Pillai, S. U.: Probability, random variables and stochastic processes.
908 McGraw-Hill. New York. 666, 1991.

909 Poulos, G. S., Blumen, W., Fritts, D. C., Lundquist, J. K., Sun, J., Burns, S. P., Nappo,
910 C., Banta, R., Newsom, R., Cuxart, J., Terradellas, E., and Balsley, Ben.: CASES-99:

911 a comprehensive investigation of the stable nocturnal boundary layer. Bull. Amer.
912 Meteor. Soc., 83, 555–581, 2002.

913 Schotanus, P., Nieuwstadt, F. T. M., and de Bruin, H. A. R.: Temperature measurement
914 with a sonic anemometer and its application to heat and moisture fluxes, Bound.
915 Lay. Meteor., 26, 81–93, 1983.

916 Stull, R. B.: An introduction to boundary layer meteorology. Kluwer Academic Publ.
917 Dordrecht. 670, 1988.

918 Uffink, J.: Boltzmann’s work in statistical physics, Stanford encyclopedia of
919 philosophy, Edward, N. Z., 2004.

920 Vickers, D., Mahrt, L.: Quality control and flux sampling problems for tower and
921 aircraft data. J. Atmos. Oceanic. Technol., 14, 512-526, 1997.

922 Webb, E. K., Pearman, G. I., and Leuning, R.: Correction of the flux measurements for
923 density effects due to heat and water vapor transfer, Q. J. R. Meteorol. Soc., 106,
924 85–100, 1980.

925 Wilczak, J. M., Oncley, S. P., and Stage, S. A.: Sonic anemometer tilts correction
926 algorithms. Bound. Lay. Meteor., 99(1), 127-150, 2001.

927 Wyngaard, J. C.: Turbulence in the atmosphere, getting to know turbulence,
928 Cambridge University Press, New York, 393 pp. 2010.

929 Zuo, H., Xiao X., Yang Q., Dong L., Chen J., Wang S.: On the atmospheric movement
930 and the imbalance of observed and calculated energy in the surface layer, Sci. China.
931 Ser. D-Earth Sci., 55, 1518-1532, 2012.

932

933

934
935

Table 1 Local Stability Parameter $(z-d)/L_c$ of the Eddies in Different Temporal Scales on 25 August

Time	3:00-4:00	7:00-8:00	14:00-15:00
Eddy scale			
≤ 2 min	0.59	0.52	-0.38
≤ 3 min	0.31	0.38	-0.44
≤ 5 min	0.28	0.16	-0.40
≤ 10 min	-0.01	0.15	-0.34
≤ 30 min	-0.04	-0.43	-0.27
≤ 60 min	-0.07	-1.29	-0.30

936

Table 2 Parameters of the Fitting Curve of MOS relation for Vertical Velocity Variance

	10 min		30 min		60 min	
	$z/L < 0$	$z/L > 0$	$z/L < 0$	$z/L > 0$	$z/L < 0$	$z/L > 0$
c_1	1.08	1.17	1.06	1.12	0.98	1.06
c_2	4.11	3.67	3.64	3.27	4.62	2.62
R	0.97	0.76	0.94	0.56	0.83	0.30
S	0.19	0.25	0.17	0.27	0.25	0.31

937

938

939

940

941

942

943

944

945

946

947

948

949

950

951

952

953

954

955

956

957

958

959

960

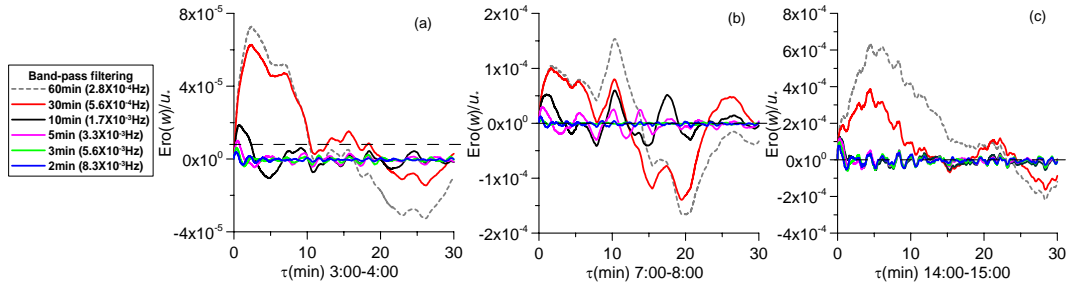


Fig. 1. Variation of mean ergodic function $Ero(w)$ of vertical velocity measured at the height 3.08 m in NSPCE with relaxation time for the different scale eddies after band-pass filtering. Panels (a), (b) and (c) are the respective results of the three time frames. If their mean ergodic function is more approximate to zero, then eddies in the corresponding temporal scale will more closely satisfy the ergodic conditions.

963

964

965

966

967

968

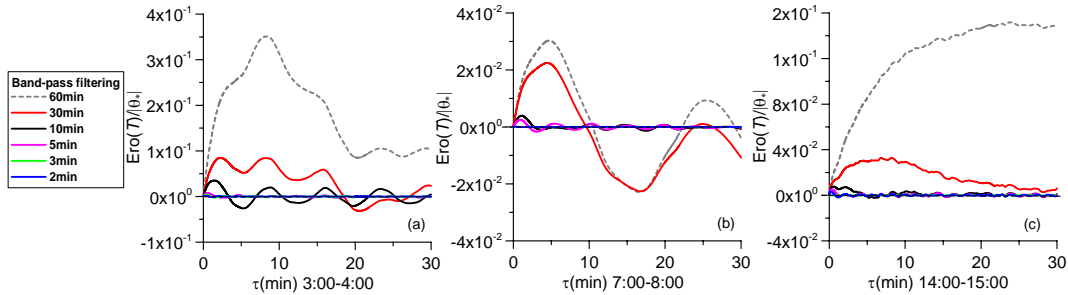


Fig. 2. Variation of mean ergodic function $Ero(T)$ of the different scale eddies of temperature with relaxation time (other conditions are as some as Fig. 2, and the same applies to the following figures).

971

972

973

974

975

976

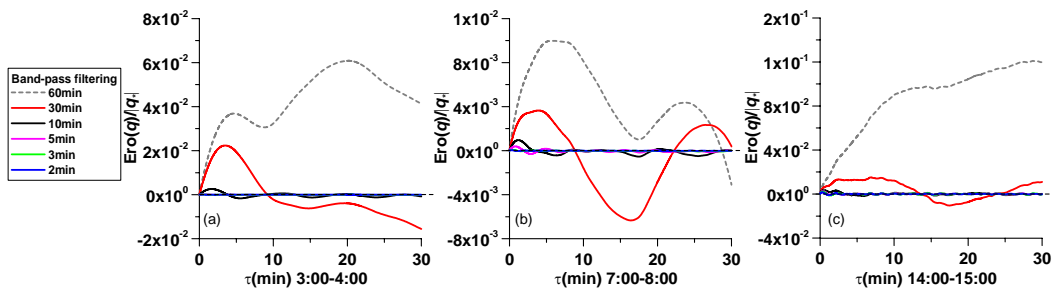


Fig. 3. Variation of mean ergodic function $Ero(q)$ of the different scale eddies of humidity with relaxation time.

977

978

979

980

981

982

983

984

985

986

987

988

989

990

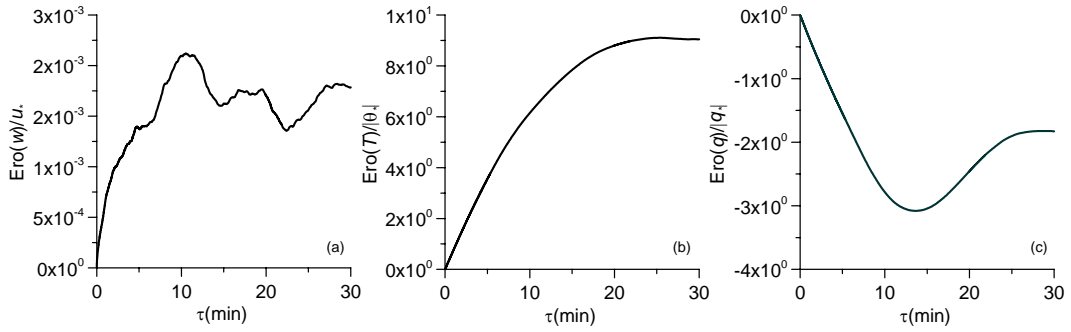
991

992

993

994

995



996

Fig. 4. Variation of mean ergodic function $Ero(w)$ of the vertical velocity (a), temperature (b) and specific humidity (c) before filtering at 14:00-15:00 (CST) during midday in NSPCE with relaxation time τ .

997

998

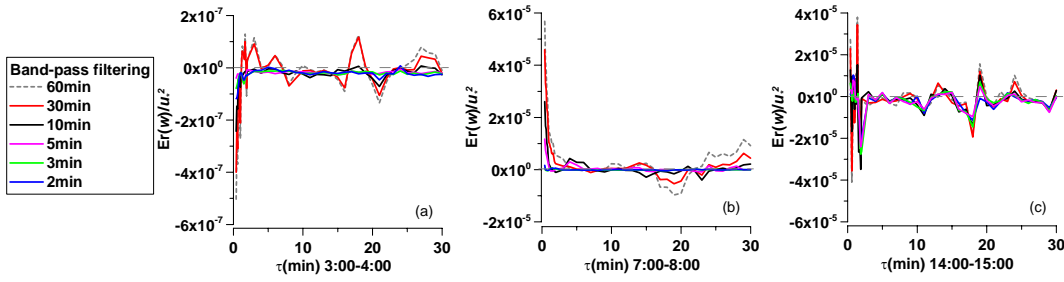
999

1000

1001

1002

1003



1004

Fig. 5. Variation of the autocorrelation ergodic function of vertical velocity with relaxation time for different scale eddies.

1005

1006

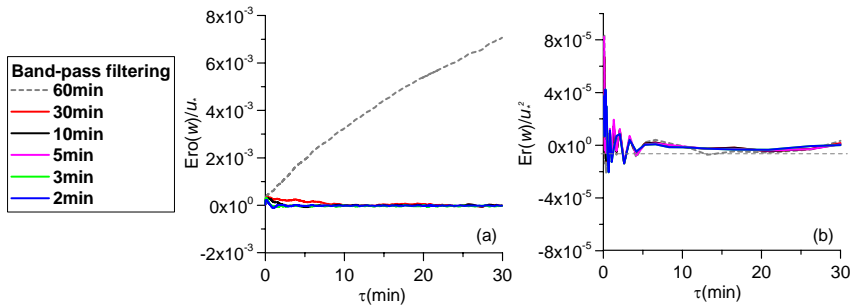
1007

1008

1009

1010

1011



1012

Fig. 6. Variation of mean ergodic function (a) and autocorrelation ergodic function (b) of the vertical velocity with relaxation time for the different scale eddies in the seven stations of CASES-99.

1013

1014

1015

1016

1017

1018

1019

1020

1021

1022

1023

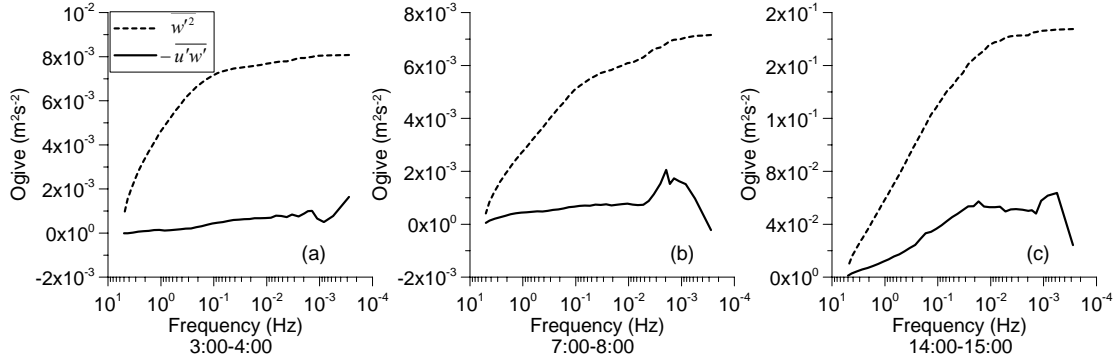


Fig. 7. Variation of Ogive functions of $\overline{w'^2}$ and $-\overline{u'w'}$ with frequency at height 3.08 m for the three time frames in NSPCE.

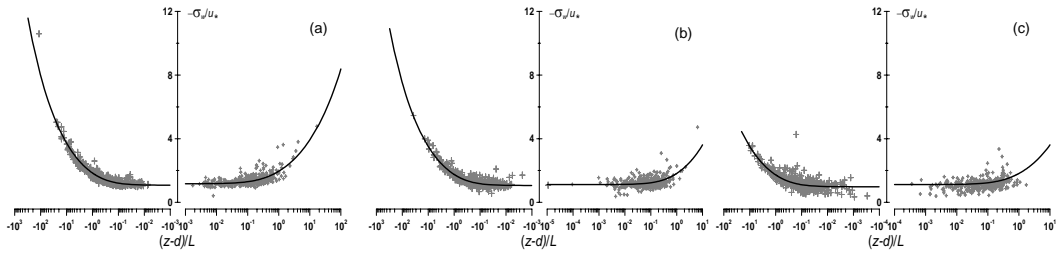


Figure 8. MOS relation of vertical velocity variances of the different scale eddies in NSPCE; Panels (a), (b) and (c) respectively represent the similarity of eddies of 10 min, 30 min and 60 min in the temporal scale.

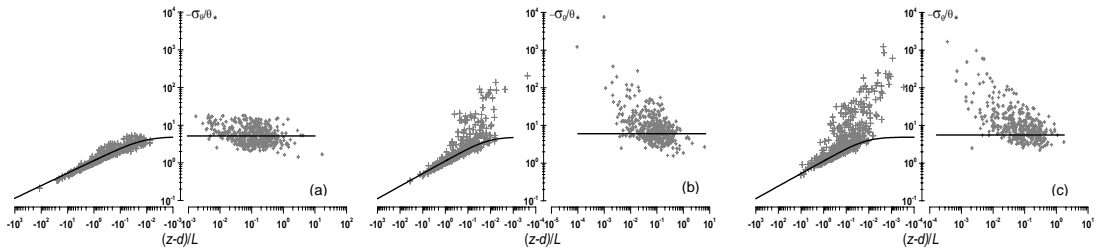


Figure 9. MOS relations of temperature variance of in different scale eddies of NSPCE; Panels (a), (b) and (c) respectively represent the similarity of the eddies of 10 min, 30 min and 60 min in the temporal scale.